

Evolution of Mechanical Properties and Energy Loss in Cement Mortar under Loading and Unloading Cycles

Abhay Anand

*Indian Institute of Science, Bangalore, India
abhayanand@iisc.ac.in*

Dr. Jyant Kumar

Indian Institute of Science, Bangalore, India

Abstract

This study presents a novel approach to investigate the mechanical behaviour of cement mortar (15% cement content) under controlled laboratory conditions. The experimental investigation consists of strain-controlled loading and unloading cycles at a constant rate of 0.01 mm/min to simulate loading unloading condition, and ultrasonic tests. Tests were conducted in five cycles of loading and unloading, with each cycle incrementally increasing the axial strain by 0.05%. During the loading-unloading tests, the maximum axial strain was restricted to 0.25%. For the loading-unloading test, samples are tested under 0 MPa, 10 MPa, and 20 MPa confining pressure to understand the influence of confinement on the material's response. Additionally, ultrasonic P and S wave tests were performed on the samples to calculate the dynamic elastic moduli.

This study investigates the stiffness and energy dissipation of cement mortar under lateral confinement. As the material accumulates plastic strain (permanent deformation), its stiffness changes during loading and unloading cycles. Interestingly, the material is observed to be stiffer when unloading compared to loading phase. By measuring the energy loss in each loading-unloading loop (area of the hysteresis loop), this study aims to understand how the mortar dissipates energy in a hysteresis loop. Additionally, the study compares the static elastic modulus measured from loading unloading tests with the dynamic elastic modulus obtained from ultrasonic tests. These findings are validated against the available data on various rock types in literature.

This study is valuable for geotechnical engineers, enabling them to better predict the behaviour of foundations, embankments, and other structures subjected to cyclic loading in real-world scenarios. The findings contribute to the development of robust laboratory testing methodologies for cement mortar and other granular materials.

Keywords

Cement mortar, Loading unloading test, Ultrasonic test, Stiffness evolution, and Energy dissipation

1 Introduction

Cement mortar is a versatile composite material used in construction field in diverse applications such as buildings, tunnels, mines, dams, etc. (Mirza and Durand 1994; Schulze 1999; Klyuev et al. 2022). These structures are undergoing severe damage due to repetitive loading as time progress in its service period. Understanding the mechanical behaviour of cement mortar is quite complex since it is highly heterogeneous in nature. The response to cyclic loading and the mechanical properties with increasing plastic strain, is essential for assessing the residual strength.



Several research are conducted to establish uniaxial compressive behaviour on cubical and cylindrical specimens have been employed to assess the stress-strain response of cement mortar (Ribeiro et al. 2016; Nalon et al. 2021). Many of literatures (Yang et al. 2015; Guo et al. 2018) are argued that, relative proportion of cement in a mortar mix can significantly influence its compressive strength and stiffness, which can be comparable with different types of rocks samples. The existing literature in uniaxial results insufficient for actual structure response since its subjected to complex loading. These complex loads include biaxial or triaxial condition, which plays a vital role in the damage mechanics of rocks. Triaxial loading studies offers a more realistic representation of the stress state experienced by structural elements. While extensive research has been conducted on the triaxial behaviour of rocks, relatively fewer studies have focused on cement mortar, particularly under cyclic loading conditions (Yurtdas et al. 2004; Kaklis et al. 2018; Jie et al. 2019).

This study focusses to investigate the stress-strain behaviour of cement mortar specimens under different confining pressures by incorporating cyclic loading and unloading phenomena under confinement. Series of triaxial experiment are conducted on cement mortar specimen by performing loading and unloading in sequential manner. These experiments are performed in unconfined and confined state (10 MPa and 20 MPa) to investigate the effect of confinement. The findings from this study will provides better understanding of the mechanical behaviour of cement mortar, enabling more accurate predictions of structural performance and facilitating the design of safer and more durable structures. This research implications could extend to rock specimens exhibiting similar mechanical behaviour in better sense.

2 Materials and specimen preparation

2.1 Materials used:

The specimens were prepared using Ordinary Portland Cement (OPC) having grade of 53, and fine sand are its primary components. The size of fine aggregates ranges from 0.07 to 1.1 mm, which indicating a poorly graded distribution as shown in Fig. 1(a). The grains were primarily angular in shape, as observed through scanning electron microscope (SEM) imaging as shown in Fig. 1(b).

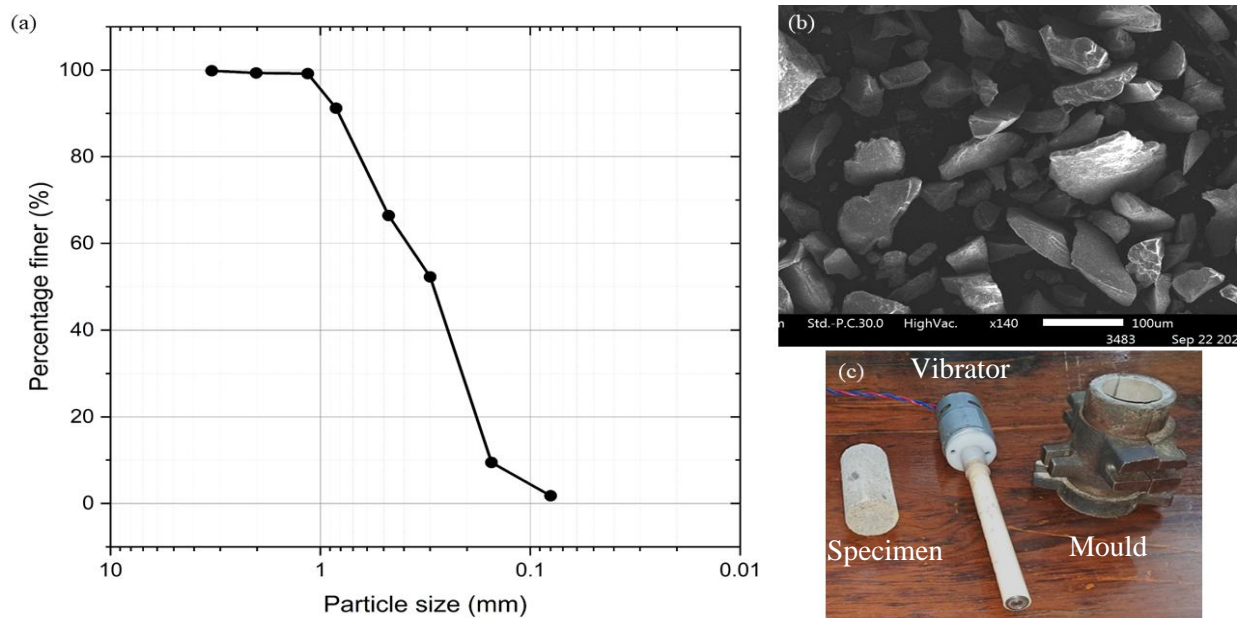


Fig. 1(a) Particle size distribution curve, (b) SEM image of the sand, (c) mould, self-made compacting vibrator, and sample after 28 days of curing period.

2.2 Specimen preparation

The cement mortar specimens are prepared as cylindrical samples having a diameter (ϕ) of 38 mm and a height (H) of 76 mm, having 15% cement content. The process of specimen preparation is explained in detail through the following step-by-step procedure:

- The sand was initially moistened with 10 ml of water to ensure even coating and better cement adhesion. Cement was then mixed into the wet sand, maintaining a water-to-cement (w/c) ratio

kept as 0.4. To account for potential water loss, an additional 5 ml of water was added and thoroughly mixed.

- Fig. 1(c) depicts, self-made vibrator for compaction and mould used to prepare the specimen. The mixture was then layered into cylindrical moulds and vibrated for 30 sec using a custom-built vibrator to ensure proper compaction and which eliminate air pockets. To ensure the interlayer bonding, top surface of each layer was scratched properly. After 24 hours, the moulds were removed, and the specimens were cured in water for 28 days. They were then sun-dried for a day to remove excess moisture.

This preparation protocol resulted in specimens with minimal variation in density and ultrasonic properties. Table 1 shows the various properties measured from ultrasonic test and material properties corresponding to 15% cement mortar, indicating homogeneity, and ensuring reliable experimental data.

Table 1 Basic properties and ultrasonic wave velocities of 15% cement mortar.

Specimens	Confining pressure (MPa)	Mass (kg/m ³)	density	P-wave velocity, V_p (km/s)	S-wave velocity, V_s (km/s)
A1	0	2017.14		2.76	1.69
A2	10	2017.32		2.83	1.74
A3	20	2016.95		2.86	1.75

3 Experimental setup and test procedure

3.1 Test setup

The loading unloading triaxial experiments were conducted using a closed loop servo-hydraulic rock triaxial testing machine equipped with a high-resolution data acquisition system (DAQ) as shown in Fig. 2(a). Fig. 2(b) illustrate the various components of cross-sectional view of actuator and load cell arrangements. The loadcell having a load carrying capacity of 1000 kN in vertical direction. A key feature of this apparatus is the additional ultrasonic sensors (piezoelectric material) attached to the top and bottom pedestals along with triaxial, allowing for the transmission and reception. These sensors measure the low-strain primary (P), and shear (S) waves. The oil-filled pressure vessel (cell pressure intensifier) enables the application of confining pressures up to 50 MPa on the specimens, facilitating measurement of waves velocities at high confining pressures.

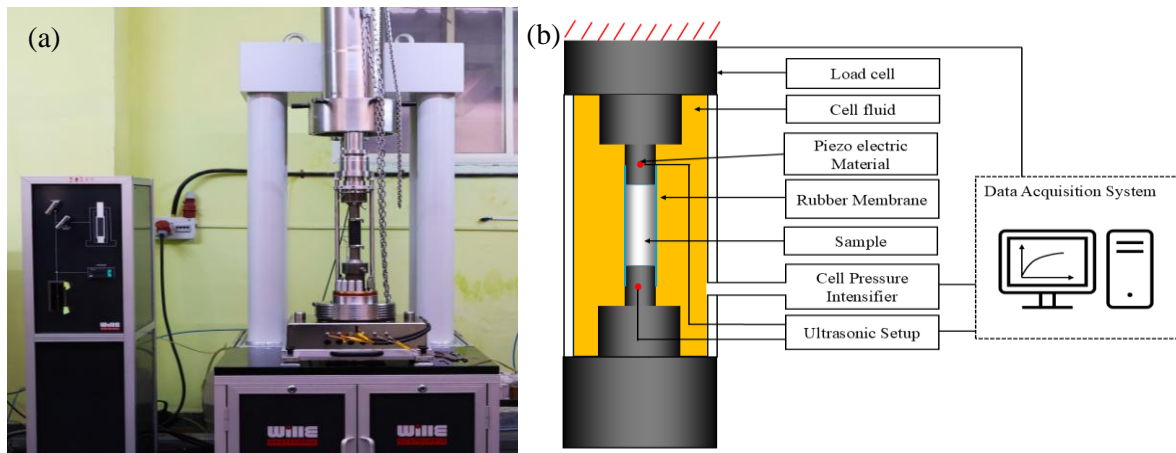


Fig. 2 (a) Image and (b) schematic diagram of the rock triaxial setup.

3.2 Experimental procedure

Preloading:

The cured cylindrical specimens are placed in the triaxial chamber, an initial stabilizing load of 2 MPa was applied to eliminate any initial slack or friction. Then the chamber was filled with hydraulic fluid, and specific confining pressures were applied hydrostatically while maintaining a constant deviatoric stress of 2 MPa. This initial condition was common to all two tests: triaxial loading-unloading, and ultrasonic tests, regardless of the confining pressure.

To study the cyclic loading and unloading two experimental protocols are used. The methodology of each protocol was explained below:

1. **Ultrasonic test:** Low-frequency P and S waves are transmitted through the specimens at different confining pressures to measure wave velocities for calculating dynamic elastic modulus (E_d). For a detailed description of the ultrasonic testing procedure, readers are referred to our previous study (Anand & Kumar, 2024).
2. **Triaxial loading-unloading test:** The specimens were subjected to loading and unloading at unconfined state and confined state corresponding to 10 MPa and 20 MPa. The loading cycles were conducted up to a strain increment of 0.05% in regular intervals with deformation rate of 0.01 mm/min, then it followed by unloading up to its initial state of stress with same deformation rate. This procedure was followed for five cycles. Each cycle consisting of additional increment of 0.05% strain.

4 Results and discussion

In this section, the outcome of loading and unloading experiments are explained in detail.

Fig. 3(a) illustrates the variation of deviatoric stress (σ_d) with axial strain (ϵ_a) for 0 MPa, 10 MPa and 20 MPa confining pressure. It is evident that as the confining pressure increases, the deviatoric stress at each strain level also rises. This demonstrates the impact of external confinement on the specimen's failure.

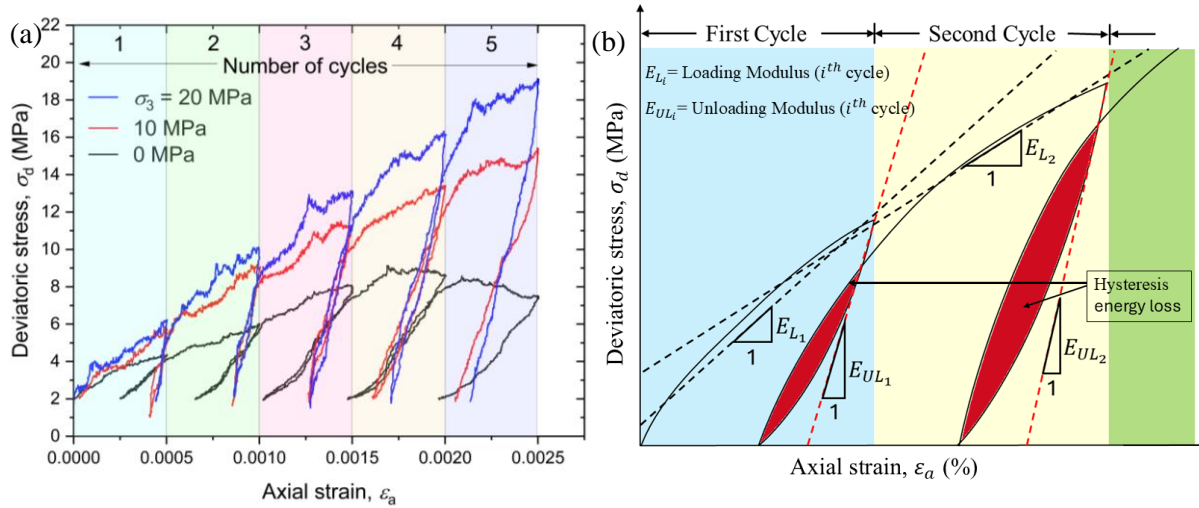


Fig. 3 (a) Variation of deviatoric stress and axial strain at different confining pressure, (b) basic terminologies related to loading unloading cycle.

Fig. 3(b) illustrate the loading and unloading features of the σ_d and ϵ_a . These terminologies associated with Fig. 3(b) are loading modulus (E_L), unloading modulus (E_{UL}), and hysteresis energy loss per unit volume are explained below:

- Loading modulus (E_L): It is the slope of the stress-strain curve in the loading phase of testing. It represents how much a material resists deformation when stress is applied.

$$E_L = \frac{\Delta\sigma_d}{\Delta\epsilon_a} \quad (\text{during loading phase}) \quad (1a)$$

- Unloading modulus (E_{UL}): The unloading modulus is the slope of the stress-strain curve during the unloading phase. It represents how the material recovers when the applied load is removed.

$$E_{UL} = \frac{\Delta\sigma_d}{\Delta\varepsilon_a} \quad (\text{during unloading phase}) \quad (1b)$$

- Hysteresis energy loss per unit volume: It is defined as the area of stress-strain curve during unloading and loading loop of each cycle. In the process of loading-unloading, it is the amount of extra energy per unit volume required to return the same stress state before unloading.

These parameters are essential to understand the loading and unloading moduli, reveals the material's stiffness and modulus of elasticity, under different loading conditions. Additionally, loss in hysteresis energy shows the energy dissipated during loading and unloading, which is essential for assessing the durability and performance.

Fig. 4 illustrates the development of plastic (ε_P) and elastic strains (ε_E) as function of axial strain (ε_a) (total strain). As increase in ε_a , the plastic strain continuously increases. It shows that under confined conditions, the material exhibits a more pronounced plastic behaviour compared to its elastic behaviour. Consequently, at higher confining pressures, the elastic strain is reduced while the plastic strain is increased.

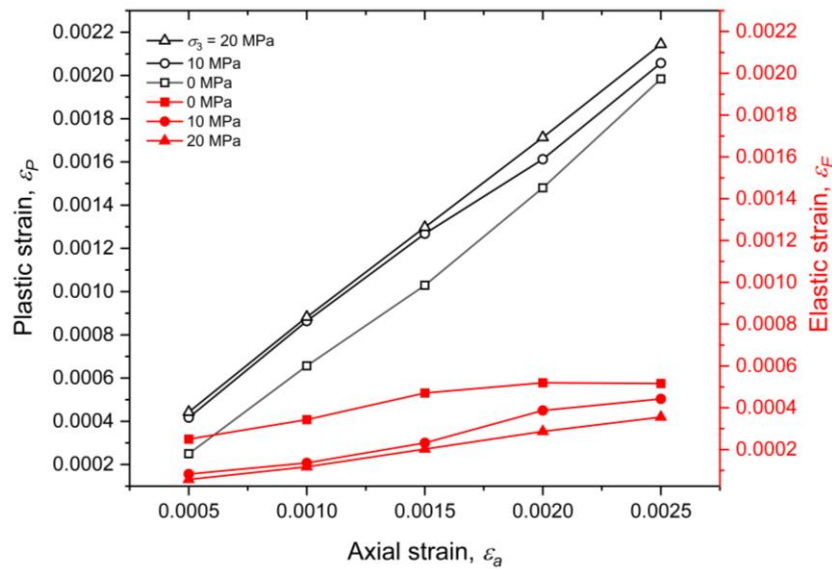


Fig. 4 Variation of plastic strain and elastic strain with change in axial strain for different confining pressure.

Fig. 5 illustrates the variation of loading and unloading modulus with plastic strain in both confined and unconfined states. In Fig. 5(a), the loading modulus in the unconfined state initially decreases, indicates the initial collapse of micro-pores. This followed by an increase in E_L , signifying the strain hardening as increased in ε_P . This peak E_L are the critical value which indicates the point of instability where the specimen losses its load carrying capacity due to formation of micro cracks which is also evident in nonlinear behaviour in Fig. 3(a). Eventually, the modulus decreases to a negative value, indicating the failure of the specimen for unconfined tested specimen. In contrast, specimen subjected to a high confining pressure of 10 MPa and 20 MPa, the initial collapse of some micro-pores has already occurred during the application of high confinement hydrostatically. Therefore, the initial decrease in loading modulus is not as pronounced as seen in the unconfined state. However, the subsequent behaviour of the loading modulus is similar to that in the unconfined state, showing an increase due to strain hardening and a final decrease indicating specimen attending to failure.

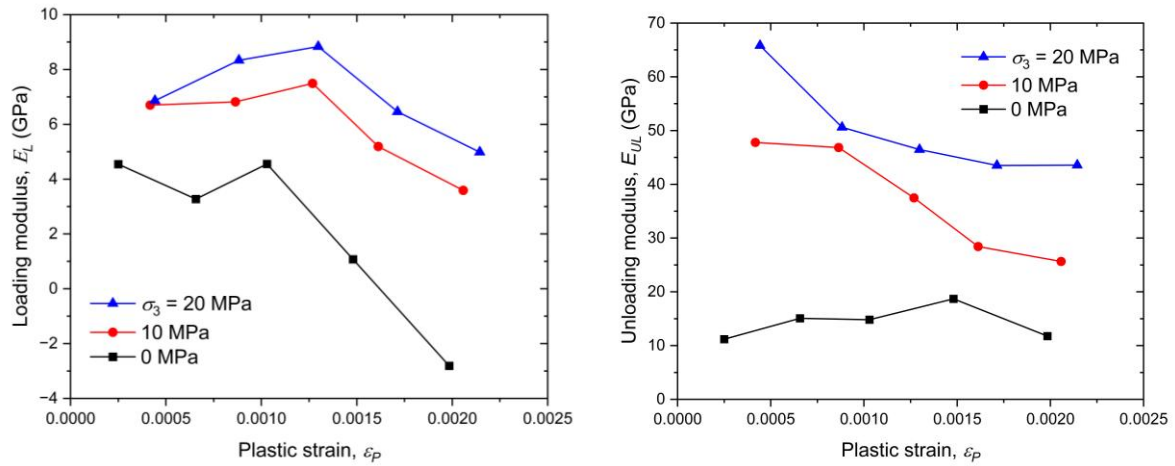


Fig. 5 Variation of (a) loading modulus and (b) unloading modulus with plastic strain at different confining pressure.

In Fig. 5(b), shows unloading modulus, expressed in ϵ_p . The slope of the stress-strain plot during unloading, increases as the plastic strain increases. This suggests that the material's strength is declining, making it less resistant to applied loads. Consequently, the material's ability to sustain deviatoric stress is decreasing rapidly. This accelerated reduction in deviatoric stress results in a higher unloading modulus. One should note that even though specimen has lost its ability to resist deviatoric stress, due to application of high confining pressure, it's not failing.

Fig. 6 shows the variation in hysteresis energy loss per unit volume, which increases more exponentially with the number of loading-unloading cycles was seen in specimen subjected under high confining pressures compared to the unconfined state, because at higher confining pressures, it is more energy required for the material to regain the same stress state after the unloading phase.

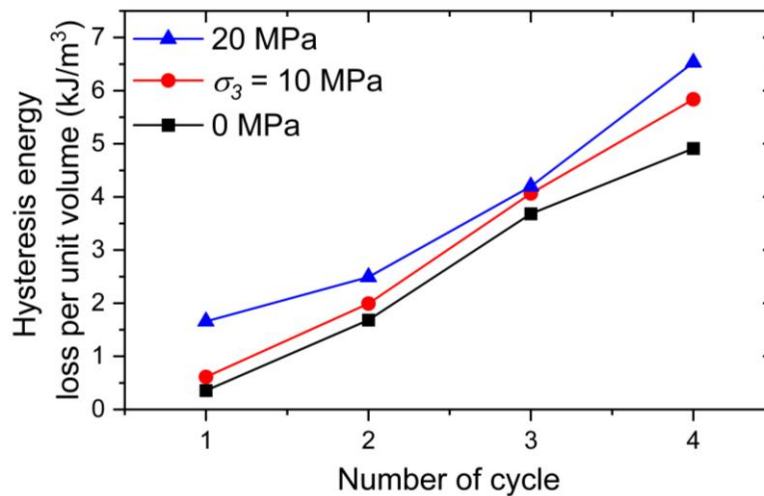


Fig. 6 Hysteresis energy loss vs number of cycle at different confining pressure.

Table 2 Comparison of static and dynamic elastic modulus of specimen with available literature.

Reference	Type of Material	Static elastic modulus, E_s (GPa)	Dynamic elastic modulus, E_d (GPa)
Present Study	Cement mortar (15% cement)	4.5-6.8	13.89-14.64
Schneider (1967)	Hard Rock	1.08-25.27	5.96-84.22
Moradian and Behnia (2009)	Marlstone (Sedimentary rock)	3.24-7.77	6.92-13.29
	Sandstone (Sedimentary rock)	0.77-9.25	9.62-25.39
	Limestone (Sedimentary rock)	1.09-90.49	4.98-83.89

Table 2 presents comparison of the static, and dynamic elastic modulus of various rock samples tested by various researchers and current study.

After knowing the values of V_p and V_s from ultrasonic test, the value of the Poisson ratio (ν) was then computed by using the following expression (Richart et al. 1970):

$$\nu = \frac{(V_p^2 - 2V_s^2)}{2(V_p^2 - V_s^2)} \quad (2a)$$

dynamic Young's modulus (E_d) were determined by using following expressions:

$$G_d = V_s^2 \rho \quad (2b)$$

$$E_d = 2G(1 + \mu) \quad (2c)$$

The table illustrates more similarities between these rock specimens and cement mortar specimens in terms of their dynamic and static elastic modulus. This study shows E_s and E_d for 15% cement mortar ranges from 4.5-6.8 *GPa* and 13.89-14.64 *GPa* respectively. The static elastic modulus is typically measured under slow or static loading, while the dynamic elastic modulus is determined under rapid or dynamic loading conditions.

By comparing these values, we can infer the material's stiffness and its ability to withstand different types of real-world stress state. Furthermore, investigation on this will provide more valuable insights for designing aspect of real field applications, to prevent catastrophic damage from cyclic loading and unloading.

5 Conclusions

In this study, triaxial loading and unloading tests were conducted on cylindrical specimen made up of cement mortar. Experimental investigations are carried out on cement mortar at two different confining pressures of 0 *MPa*, 10 *MPa*, and 20 *MPa* respectively with loading and unloading up to five repetitive cycles. Additionally, ultrasonic tests were conducted to measure P and S wave velocities, which were then used to determine the dynamic elastic modulus. The following major conclusions are drawn from this investigation are as follow:

1. The specimen under higher confining pressure losses its elastic behaviour and shows more ductile behaviour, whereas at unconfined state the specimens are brittle.
2. The increase in plastic strain, the loading modulus shows a sudden drop due to the closing of micro-pores then it increases to reach critical modulus. This value considered material property, since beyond this steady degradation occurs due to accumulation of damage in specimen. The unconfined samples undergo more damage compared to the specimen at 10 *MPa* and 20 *MPa* due to confinement.
3. The elastic modulus, associated with the unloading segment of the stress-strain curve, consistently exceeds the corresponding loading modulus. An increase in confining pressure results in a continuous rise in the unloading modulus.
4. Hysteresis energy loss during a loading-unloading-reloading cycle increases progressively with the number of cycles. It increases at higher confining pressures.
5. Dynamic elastic moduli values, derived from ultrasonic tests, are consistently higher than the loading modulus values obtained from triaxial tests which is in well agreement with the values reported in the literature.
6. The similarities observed in Table 2 suggest that cement mortar specimens can be used as a proxy for certain rock types in engineering applications, providing a cost-effective and practical alternative for experimental studies and simulations.

While this study focuses on cement mortar, the findings have potential applications for rocks with elastic moduli and compressive strengths like those of the specimens used in this investigation.

References

1. Schneider B (1967) Contribution à l'étude des massifs de fondation de barrages. Institut. Dolomieu (géologie)
2. Richart FE, Hall JR, & Woods RD (1970) Vibrations of soils and foundations.
3. Mirza J, Durand B (1994) Evaluation, selection and installation of surface repair mortars at a dam site, *Constr. Build. Mater.* vol. 8 (Jan. 1994) 17–25, [https://doi.org/10.1016/0950-0618\(94\)90004-3](https://doi.org/10.1016/0950-0618(94)90004-3)
4. Yurtdas I, Burlion N, Skoczylas F (2004) Triaxial mechanical behaviour of mortar: Effects of drying, *Cem. Concr. Res.* vol. 34 1131–1143, <https://doi.org/10.1016/j.cemconres.2003.12.004>
5. Moradian Z, Behnia M (2009) Predicting the uniaxial compressive strength and static young's modulus of intact sedimentary rocks using the ultrasonic test, *International Journal of Geomechanics* vol. 9 14–19, [https://doi.org/10.1061/\(asce\)1532-3641\(2009\)9:1\(14\)](https://doi.org/10.1061/(asce)1532-3641(2009)9:1(14))
6. J. Schulze(1999) Influence of water-cement ratio and cement content on the properties of polymer-modified mortars, *Cem. Concr. Res.* vol. 29, 909–915, [https://doi.org/10.1016/S0008-8846\(99\)00060-5](https://doi.org/10.1016/S0008-8846(99)00060-5)
7. Yang SQ, Ranjith PG, Huang YH, Yin PF, et al. (2015) Experimental investigation on mechanical damage characteristics of sandstone under triaxial cyclic loading, *Geophys. J. Int.* vol. 201 662–682 <https://doi.org/10.1093/gji/ggv023>
8. Ribeiro D, Néri R, Cardoso R (2016) Influence of water content in the UCS of soil-cement mixtures for different cement dosages, *Procedia Eng.* vol. 143 59–66, <https://doi.org/10.1016/j.proeng.2016.06.008>
9. Kaklis K, Agioutantis Z, Mavrigiannakis S, Maravelaki-Kalaitzaki P (2018) On the experimental investigation of pozzolanic lime mortar stress-strain behavior and deformation characteristics when subjected to unloading-reloading cycles, *Procedia Struct. Integr.* vol. 10 129–134, <https://doi.org/10.1016/j.prostr.2018.09.019>
10. Guo H, Ji M, Zhang Y, Zhang M (2018) Study of mechanical property of rock under uniaxial cyclic loading and unloading, *Adv. Civ. Eng.* vol. 2018 1–6 <https://doi.org/10.1155/2018/1670180>
11. Jie W, Song W, Cao S, Tan Y (2019) Mechanical properties and failure modes of stratified backfill under triaxial cyclic loading and unloading, *Int. J. Min. Sci. Technol.* vol. 29 809–814, <https://doi.org/10.1016/j.ijmst.2018.04.001>
12. Nalon GH, Alves MA, Pedroti LG, Ribeiro JCL, et al. (2021) Compressive strength, dynamic, and static modulus of cement-lime laying mortars obtained from samples of various geometries, *J. Build. Eng.* vol. 44 <https://doi.org/10.1016/j.job.2021.102626>
13. Klyuev S, Klyuev A, Fediuk R, Ageeva M, et al. (2022) Fresh and mechanical properties of low-cement mortars for 3D printing, *Constr. Build. Mater.* vol. 338 127644– 388 127644, <https://doi.org/10.1016/j.conbuildmat.2022.127644>
14. Anand A, Kumar J (2024) Effect of High Confining Pressure on Ultrasonic Wave Velocities and Elastic Moduli of Cemented Sand, *Trans Indian Natl. Acad. Eng.* Vol. 9, 501–513 (2024). <https://doi.org/10.1007/s41403-024-00475-6>